Predicting Vibrational Mean Free Paths in Amorphous Materials

Jason M. Larkin[1] and Alan J. H. McGaughey[1]

[1]*Department of Mechanical Engineering*
Carnegie Mellon University
Pittsburgh, PA 15213

(Dated: June 14, 2013)

Understanding thermal transport in crystalline systems requires detailed knowledge of phonons, which are the quanta of energy associated with atomic vibrations. By definition, phonons are non-localized vibrations that transport energy over distances much larger than the atomic spacing. For disordered materials (e.g., alloys, amorphous phases), with the exception of very long wavelength modes, the vibrational modes are localized and do not propagate like phonons. The Einstein model assumes that the mean free path of these localized vibrations is the average interatomic distance and that their group velocity is equal to the speed of sound. The Cahill-Pohl model assumes that the mean free path of the localized modes is equal to half of their wavelength. While these approach can be used to estimate the thermal conductivity of disordered systems, they only provide a qualitative description of the vibrations that contribute to the lattice thermal conductivity. Using lattice dynamics calculations and molecular dynamics simulations on model amorphous silicon and silica, we predict and characterize the contributions from phonons and localized vibrations to lattice thermal conductivity. The vibrational mean free paths are predicted for these two amorphous materials and the thermal conductivity accumulation function is compared with recent experimental results.

I. INTRODUCTION

Thermal transport at scales comparable to phonon wave- lengths and mean free paths (MFPs) is presently a topic of considerable interest [14].[1–4]

Recently, nanostructured materials such as nanowires, superlattices, and nanocomposites with strongly reduced thermal conductivities due to phonon scattering at interfaces and boundaries have been reported and are being assessed for use in thermoelectrics applica- tions [3,4,6,7].[3–6]

Another type of size effect can occur if there is a temperature gradient over length scales compa- rable to phonon MFPs. In this case, local thermal equilib- rium does not exist and the transport is nondiffusive.

Transient ballistic transport has been studied using heat- pulse techniques at cryogenic temperatures [8].[?]

A nonlocal theory of heat transport was proposed as a modification of diffusion theory [9].[7]

It was also predicted that the heat conduction from a nanoparticle is significantly reduced from the Fourier law prediction.[8]

raditionally, empirical expressions and simple relaxation time models have been the only means to estimate MFPs [11].[9]

Recent first-principles calculations show that MFPs of phonons relevant to thermal conduc- tivity vary by more than 5 orders of magnitude [12].[10]

Experimentally, inelastic neutron scattering has been used to measure phonon lifetimes in certain materials, but this technique is more suited for single crystal samples [13].[11]

An x-ray diffraction and thermoreflectance technique can measure ballistic transport in some structures [14].[12]

Koh et al. proposed a technique which uses a variation of modulation frequency to measure MFPs, but this technique is limited by the modulation frequency [15].[13]

hermal conductivity (k), which relates the heat flux (! q) and temperature gradient (rT) in a material through the Fourier law, ! q 14 krT, results from the cumulative contributions of phonons with a broad range of mean free paths (MFPs). The spectral MFP distribution is critical in nanostruc- tured materials and devices, where size effects selectively scatter phonons or create non-Fourier conduction based on individual phonon MFPs. Such effects have an impact on heat dissipation in nanoelectronics and photonics, as well as the design of nanostructured thermoelectric materials with reduced thermal conductivity19. Because of its ubiquity in electronics, crystalline silicon (c-Si) has emerged as the prototypical material of study, yet controversy persists on what phonon MFPs dominate thermal transport, even in the bulk material. Kinetic theory defines the thermal conductivity as k 14 Cvs LG =3, where C is the volumetric heat capacity, vs is the speed of sound and LG is the average (or grey) MFP. For c-Si, kinetic theory yields LG 14 41 nm at a temperature (T) of 300 K10. This grey approximation severely underestimates the MFPs of the phonons that contribute significantly to thermal conductivity because (i) dispersion makes vs an overestimate of the average group velocity of acoustic phonons and (ii) optical phonons contribute to C but negligibly to bulk k (ref. 11). Thermal conductivity measurements of thin silicon films indicate that an effective MFP of 300 nm at T 14 300 K is more appropriate12.

The thermal conductivity of amorphous solids display unique temperature dependance compared to ordered

solids.[14] Cahill argued that the lattice vibrations in a disordered crystal are essentially the same as those of an amorhous solid.[15]

Measurements by all the refs from Galli paper, including Moon.[16–22] The key to understanding such measurement is to estimate a MFP for the vibrational modes in disordered systems.

The goal of this work is to predict the MFP of vibrational modes in disordered systems. Simple Lennard-Jones systems will be studied. A perfect LJ crystal are alloyed with a species of differing mass and amorphous samples are prepared. Thermal transport will be studied to quantify and characterize the ordered and disordered contributions to lattice thermal conductivity. In particular, a more rigorous way to classify vibrational modes in disordered alloys and amorphous samples as phonon-like or diffuson will be investigated. These results will be compared to the phenomenological Einstein and Cahill-Pohl models,? ? ? .

The vibrational modes in these systems are characterized in the limit of propagating (phonon) and non-propagating (diffuson) modes by predicting the mode lifetimes and estimating their mean free paths. Estimating an effective dispersion relation is necessary for calculating an effective group velocity for disordered, which is crucial for transforming lifetimes to MFPs. The spectrum of phonon MFPs and the accumulated thermal conductivity are predicted for a model of amorphous silicon. Predictions of thermal conductivity using a boundary scattering model demonstrates

Measurements of a-Si thin films demonstrate a film-thickness dependance of the thermal conductivtiy.

[16] find 1.8 W/m-K, similar to the SW results presented here.

Yang et al find as high as 7 W/m-K.[18]

Liu et al. find a film dependanc between 60 and 80 microns.[22] Claim the HWCVD method and hydrogenation creates the most ordered a-Si.

zink shows no plateau at low T for a-Si thin film, indicating the scattering of long-wavelength phonon-like modes by the boundaries.[17]

Show film thickness dependance up to 10 microns.[20]

4.8 W/m-K.[23]

minnich tudies c-Si[24]

The understanding of the accumulation function for bulk crystalline has made significant advancement experimentally and theoretically.[25] However, understanding of accumulation in amorphous systems is still not well understood.[26–28]

recent measurements of the accumulation function by Regner .[29]

Measurements of the thermal condutivity of a-SiO_2 thin films show no significant dependance on the film thickness.[30,31]

II. THEORETICAL FORMULATION

A. Thermal Conductivity

To calculate the total vibrational thermal conductivity k_{vib}, we predict the contributions from k_{ph} and k_{AF},

$$k_{vib} = k_{ph} + k_{AF}, \tag{1}$$

where k_{ph}? is the contribution from phonons or phonon-like modes and k_{AF} is the contribution from the Allen-Feldman theory of diffusons.[26,27] A study of disordered Lennard-Jones argon and Stillinger-Weber silicon lattices demonstrated that k_{AF} is a significant fraction of k_{vib}, even when spatial disorder is not included.

For amorphous systems, the spatial disorder creates strong scattering, and k_{vib} tends to be much smaller than the crystalline phase.(cite) For Lennard-Jones argon, $k_{vib} \approx k_{HS}$ For example, the thermal conductivity at 300 K is 1-6 W/m-K and 1.8 W/m-K for a-Si and a-SiO2, which k_{HS} = .(cite)

The relative contribution of k_{ph} and k_{AF} to k_{vib} has been estimated to be approximately equal for a model of a-Si at 300 K,[33] while earlier studies find that k_{ph} is less than half.[26,27] Experimental measurements and estimates show that the contribution from k_{ph} is 40%.[22]

The themal conductivity of a-GeTe[64] The thermal conductivity of silicon nanowires[45]

To calculate the total vibrational thermal conductivity k_{vib}, we predict the contributions from k_{ph} and k_{AF}. We use a Debye model for k_{ph}? and the Allen-Feldman theory of diffusons for k_{AF}[26,27] The phonon contribution is

$$k_{ph} = \frac{1}{V}\int_0^{\omega_{cut}} d\omega DOS(\omega)C(\omega)D(\omega) \tag{2}$$

and the AF diffuson contribution is

$$k_{AF} = \frac{1}{V}\sum_{\omega_i > \omega_{cut}} C_i(\omega)D_{AF,i}(\omega) \tag{3}$$

The cut-off frequency ω_{cut} identifies the transition from phonon-like to diffuson modes.[22,26,27] While this transition is not universal for various materials and material properties, phonon-like behavior can be identified for a-Si and not a-SiO_2 in this work and others, both experimentally[18,22,24,29] and numerically.[26,27,33?] Identifying this phonon-like behavior for a-Si is not sensitive qualitatively to the choice of model[22,26,27] or ω_{cut}.[18,22,26,27,45]

III. PHONONS

For a perfect lattice, all vibrational modes are phonon modes, which by definition are delocalized, propagating plane waves.[34] In an amorphous system, only in the low-frequency, long-wavelength limit are the vibrational

modes phonons. In this work, we identify the phonon limit by ω_{cut} in Eq. , which is determined in Section . By identifying ω_{cut} the contribution of phonon-like modes in a-Si and a-SiO_2 is quantified and the thermal conductivity accumulation is predicted in Section .

Using the single-mode relaxation time approximation[34] to solve the Boltzmann transport equation gives Eq. , which is the kinetic theory of a phonon gas.(cite) Further assumed in Eq. are isotropy and a single phonon polarization,(cite) making the properties a function of the mode frequency ω only.

The phonon specific heat $C(\omega)$ is taken to be

$$D(\omega) = B\omega^{-2} \tag{4}$$

Because we use molecular dynamics (MD) simulations, we

Since MD simulations are classical and obey Maxwell-Boltzmann statistics,[?] the volumetric specific heat is k_{B}/V per mode in the harmonic limit, where V is the system volume. This harmonic approximation has been shown to be valid for LJ argon and SW silicon at the temperatures of interest here[54?] and is used so that direct comparisons can be made between the MD- and lattice dynamics-based methods.

In general, the thermal conductivity k_{ph} and group velocity v_g depend on the spatial direction $\mathbf{n}$. Since the amorphous materials studied in this work are isotropic, k_{ph} and v_g are scalar quantities indepdent of the direction $\mathbf{n}$.

$$D(\omega) = B\omega^{-2} \tag{5}$$

$$D(\omega) = \frac{1}{3} v_g^2 \tau(\omega) \tag{6}$$

$$D(\omega) = \frac{1}{3} v_g \Lambda \tag{7}$$

The vibrational mean free path (MFP),

$$\Lambda(\boldsymbol{\kappa}_\nu) = v_g^2 \tau, \tag{8}$$

is the distance the phonon travels before scattering. The transformation from lifetime to MFP requires a group velocity.

Under the Debye model, which assumes isotropic and linear dispersion $v_g = v_s$, the denisty of states $DOS(\omega)$ is

$$DOS(\omega) = \frac{3\pi\omega^2}{2v_{s,DOS}^3}, \tag{9}$$

where v_s is an appropriate sound speed (see Section).(cite)

IV. DIFFUSONS

For disordered systems, the vibrational modes are no longer pure plane-waves (i.e., phonon modes), except in the low-frequency (long-wavelength) limit. When applied in the classical limit, the Allen-Feldman (AF) theory computes the contribution of diffusive, non-propagating modes (i.e., diffusons) to thermal conductivity[32]

$$k_{AF} = \sum_{diffusons} \frac{k_{\mathrm{B}}}{V} D_{AF,i}(\omega_i), \tag{10}$$

where $D_{AF,i}$ is the mode diffusivity and ω_i is the frequency of the ith diffuson. The diffusivity of diffusons can be calculated from harmonic lattice dynamics theory.[26,27,32]

$$k_{ph} = \sum_{\boldsymbol{\kappa}} \sum_{\nu} c_{ph}(\boldsymbol{\kappa}_\nu)\, \boldsymbol{v}_g^2(\boldsymbol{\kappa}_\nu)\, \tau(\boldsymbol{\kappa}_\nu)\,. \tag{11}$$

For Eq. , the sum is over the phonon modes in the first Brillouin zone, $\boldsymbol{\kappa}$ is the wave vector, and ν labels the polarization branch. The phonon mode has frequency $\omega(\boldsymbol{\kappa}_\nu)$, volumetric specific heat $C_{ph}(\boldsymbol{\kappa}_\nu)$, group velocity vector $\boldsymbol{v}_{g,\mathbf{n}}(\boldsymbol{\kappa}_\nu)$, and lifetime $\tau(\boldsymbol{\kappa}_\nu)$.

Because there is a spectrum of vibrational modes in cyrstalline and amorphous systems, there are typically a range of vibrational MFPs.(cite) By reducing the system feature sizes, the vibrational MFPs can be reduced due to boundary scattering.(cite)

Taking the phonon mode specific heat to be $c_{ph}(\boldsymbol{\kappa}_\nu) = k_B$, the phonon mode specific vibrational conductivity (Eq. (**??**)) can be written as

$$k_{ph,\mathbf{n}} = \sum_{\boldsymbol{\kappa}} \sum_{\nu} k_B D_{ph}(\boldsymbol{\kappa}_\nu)\,, \tag{12}$$

and the vibrational conductivity is determined by the phonon mode diffusitivies, defined as

$$D_{ph}(\boldsymbol{\kappa}_\nu) = v(\boldsymbol{\kappa}_\nu)^2\, \tau(\boldsymbol{\kappa}_\nu)\,. \tag{13}$$

By using lattice dynamics calculations and molecular dynamics simulations, we predict the inputs to Eq. in Section and the thermal conductivity k_{vib} in Section . The MFPs of phonons and diffusons is predicted from Eqs. and , and the thermal conductivity accumulation is predicted in Section

A. Thermal Diffusivity Limits

In the low-frequency, long-wavelength limit, the mode thermal diffusivity has the form of Eqs. eqref or eqref .(cite) The mode diffusivities generally decrease with increasing frequency,(cite) often reaching a plateau,(cite)

and then decrease exponentially to zero as the modes become localized.(cite) It is useful to consider a high-scatter limit for the mode diffusivity,

$$D_{HS} = \frac{1}{3} v_s a, \tag{14}$$

where it is assumed that all vibrational modes travel with the sound speed, v_s, and scatter over a distance of the lattice constant, a. This diffusivity assumption leads to a high-scatter (HS) limit of thermal conductivity in the classical limit[35]

$$k_{HS} = \frac{k_\mathrm{B}}{V_b} b v_s a, \tag{15}$$

where V_b is the volume of the unit cell and b is the number of atoms in the unit cell.

For mode lifetimes which depend on frequency, the Ioffe-Regel (IR) limit is

$$\tau = \frac{2\pi}{\omega}. \tag{16}$$

Assuming linear dispersion ($i.e., \omega = v_s k$), the IR limit for MFP is

$$\Lambda = \lambda, \tag{17}$$

where λ is the wavelength of the vibrational mode. These limits are not equivalent if the group velocity is mode-dependent. Also, it is generally not possible to assign a unique wavenumber to disordered modes.(cite) The IR and HS limits are examined in Section and Section .

For amorphous systems, the spatial disorder creates strong scattering, and k_{vib} tends to be near the high-scatter limit k_{HS}.(cite) It was demonstrated by Kittel that the thermal conductivity of glasses above 20 K could be interpreted using a temperature-independent high-scatter diffusivity on the order of Eq. . Since this corresponds to a phonon model with MFP $\Lambda = a$, too small to justify use of the model, implies that the dominant modes in most glasses are diffusons and not phonons.(cite)

One way to interpret this result is to use assume $k_{vib} = k_{AF} = k_{HS}$. Amorphous Lennard-Jones argon is dominated by high-scatter modes,[59] as is a model of a-GeTe, and both their $k_{vib} \approx k_{HS}$.[64] For a-SiO_2, $k_{vib} \approx 2k_{HS}$, while it is unclear what the appropriate lattice constant a should be.(cite) For a-Si, the thermal conductivity at 300 K $k_{vib} \approx (1-6)k_{HS}$, indicating that there may be a large contribution from k_{ph}.

While Eqs. and are commonly used to establish a high-scatter limit for diffusivity and thermal conductivity, predictions for a-SiGe alloys demonstrated that these are not true high-scatter limits.[26] Recently, the thermal conductivity of several materials has been measured to be significantly below k_{HS}.(cite)

V. CALCULATION DETAILS

A. Sample Preparation

1. Amorphous Si

For a-Si, we use models created by the Wooten-Winer-Weaire (WWW) algorithm in Ref. 36. Sample sizes with N_a = 216, 1000, 4096, and 100,000 were provided, where N_a are the number of atoms in the disordered supercell.(cite) A large sample was created from the $N_a = 100,000$ sample by treating it as a unit cell and tiling twice in all directions to create an $N_a = 800,000$ sample with box size L nm. All a-Si structures used have a density ρ equivalent to the perfect crystal with a lattice constant of a =5.43 $\mathring{A}$.(cite)

The Stillinger-Weber potential is used with these samples. The samples were annealed at a temperature of 1100 K for 5 ns to remove meta-stability. Amorphous materials have many different atomic (potential energy) configurations with nearly equivalent energies.(cite) The removal of meta-stability is demonstrated by an increase in the predicted sound speeds, $v_{s,T}$ and $v_{S,L}$, after annealing (see Table). This meta-stability can cause errors when predicting vibrational lifetimes using Normal Mode Decomposition (NMD, see Section).(cite)

Similar structures and results can be obtained with a-Si samples created using a melt-quench-anneal procedure,(cite) similar to that used to create a-SiO_2 samples in Section .

(footnote)In an amorhous material, there are many potential energy configurations (atomic positions) which are nearly equivalent in energy. At a sufficient temperature, the meta-stable configurations cause the equillibrium atomic positions to vary in time. This can effect on the prediction of the vibrational mode lifetimes when using the normal mode decomposition method. In the time domain, the average normal mode potential and kinetic energy must be calculated and subtracted from the normal mode energy autocorrelation function.(cite) If the average energy is not specified correctly, unphysically large or small mode lifetimes can be predicted.(cite)

(footnote) The entire procedure is performed at constnat volume. Crystalline silicon (c-Si) is first melted at a temperature of 10,000 K. The liquid is then quenched instantaneously to 300 K, and then annealed at 1100 K for 10 ns to remove meta-stability.

2. Amorphous SiO_2

The a-SiO_2 samples are used from Ref. **?** and have size N_a = 288 , 576, and 972. The atomic potentials used for a-SiO_2 are the same as in Ref. **?** except the 24-6 Lennard-Jones potential is changed to a 12-6, which has a negligible effect on the predictions presented in this paper. Larger systems of N_a = 2880, 4608, and 34562 are

created by a similar melt-quench technique as that used in Ref. **?**

(footnote) The entire procedure is performed at constant volume. Crystalline silicon (c-Si) is first melted at a temperature of 10,000 K. The liquid is then quenched instantaneously to 300 K, and then annealed at 1100 K for 10 ns to remove meta-stability.

B. Simulation Details

Molecular dynamics simulations are performed using the disordered a-SiO_2 and a-Si supercells described in Sections and . The MD simulations were performed using LAMMPS[37] with time steps of dt = 0.00905 , 0.0005 for a-SiO_2 and a-Si. Ten MD simulations with different initial conditions were run for 2^21 time steps and the atomic trajectories sampled ever 2^8 time steps. For the GK method, the thermal conductivity k_{GK} is predicted by window averaging the integral of the heat current autocorrelation function (HCACF).(cite) For a-SiO_2 and s-Si, a interval of the the HCACF integral can be found which is constant within the statistical noise.(cite) Large system sizes up to N_a = 34,000 and 800,000 can be used to predict k_{GK} for a-SiO_2 and a-Si (see Section). For smaller systems, the trajectories from the MD simulations used for the GK method are also used in the NMD method to predict the vibrational mode lifetimes (Section).

For the amorphous supercells studied, the only allowed wave vector is the gamma-point (i.e., $\boldsymbol{\kappa} = 0$), where $\boldsymbol{\kappa}$ is the wavevector and there are $3N_a$ polarization branches labeled by ν. Calculation of the vibrational modes at the Gamma point require the eigenvalue solution of a dynamical matrix of size $(3N_a)^2$ that scales as $[(3N_a)^2]^3$, limiting the system sizes that can be considered to N_a = 4608 and 4096 for a-SiO_2 and a-Si. This eigenvalue solution is also required to perform the NMD (see Section **??**) and AF calculations (see Section VII D). The frequencies and eignvectors were computed using harmonic lattice dynamics calculations and GULP.[38] The calculation of the AF diffuson thermal diffusivities (Eq.) is performed using GULP and a Lorentzian broadening of $5\delta\omega_{avg}$ and $14\delta\omega_{avg}$ for a-Si and a-SiO^2, where $\delta\omega_{avg}$ is the average mode frequency spacing.(cite) Varying the broadening around these values does not change the resulting thermal conductivity k_{AF} significantly (see Section).

VI. VIBRATIONAL PROPERTIES

A. Density of States

In this section, we discuss the frequencies and density of states (DOS) for the vibrational modes of a-SiO_2 and a-Si described in Section and . The vibrational DOS is computed by

$$DOS(\omega) = \sum_i \delta(\omega_i - \omega), \tag{18}$$

where a unit step function is used to broaden $\delta(\omega_i - \omega)$.(cite) The DOS for a-$SiO_2$ and a-Si are plotted in Fig. using two values of broadening, $10\delta\omega_{avg}$ and $100\delta\omega_{avg}$. Because of the finite model size, the low-frequency modes are sparse and the DOS has a large variability dependent on the broadening.[27] As the system size L is increased, the lowest frequency mode will continue to decrease and the gaps in frequency will fill in.(cite) The DOS for a-Si is similar to the DOS of crystalline silicon,[45**?**] particularly at low-frequency, and with pronounced features like in disordered lattices.[49,59] The DOS for a-SiO_2 is essentially constant over most of the frequency-range, except at the lowest frequencies.

While the DOS has a large amount of variability at low frequency, there is a clear scaling of $DOS \propto \omega^{-2}$ for both a-Si and a-SiO_2. The range of this scaling is larger for a-Si than a-SiO_2. By fitting the DOS from Fig. to Eq. , a sound speed is predicted at reported in Table . For both a-Si and a-SiO_2, the sound speeds predicted from the DOS are close to the transverse sound speeds predicted from the elastic constants and the structure factor. The Debel model (Eq.) predicts that the contribution from the larger longitudinal sound speed compared to the smaller transverse sound speed will scale as the difference cubed. For a-Si, the contribution from longitudinal modes to the Debye DOS is nearly an order of magnitude less than the transverse modes for a given frequency interval. For a-SiO_2, the logitudinal and transverse sound speeds are closer.(cite experimental a-DOS)

The DOS predicted for jammed systems are similarly dominated by the transverse sound speed,[50] while results for disorded lattices demonstrate[49,59]

B. Group Velocity

For a disordered solid, the three acoustic group velocities (two transverse and one longitudinal) can be predicted using the elastic constants[38] or by finite differencing of the three lowest frequency branches of the dispersion relation of the supercell.[28,33] Except for this low-frequency behavior, there is not an accepted method to predict the group velocity of a vibrational mode in a disordered system, although there have been attempts.[28,33,35,44,45] In the Cahill-Pohl (CP) model, for example, the group velocity of all disordered modes is the sound speed, v_s, which is also assumed for the HS model, Eq. (15).[35] This assumption is not generally valid for any material.[27,28,33,44,45]

Freeman gives 4100 m/s for a-SiO_2[14] 3,700 5,100 from[39] for a-Si 3,800-4,800[39] Experimentally measured values of sound speed for a-Si are 4,160[40] and 4,290 m/s[41].[42]

1. From Elastic Constants and DOS

The transverse and logitudinal sound speeds of a material can be related to the material's elastic constants, which determine the bulk (G) and shear (K) moduli.(cite) The transverse sound speed is given by(cite)

$$v_{s,T} = \frac{G}{\rho}^{1/2}, \tag{19}$$

and the longitudinal by

$$v_{s,L} = \frac{4G + 3K}{3\rho}^{1/2}. \tag{20}$$

We use the bulk and shear moduli defined in terms of the elastic constants according to the Voight convention.(cite) The sound speeds calculated from the elastic constants are reported in Table . It is clear that the DOS of our models for a-Si and a-SiO_2 are characterized by using the transverse sound speeds, rather than an averaging of the transverse and longitudinal,

$$v_s = \frac{1}{3}v_{s,L} + \frac{1}{3}v_{s,T}. \tag{21}$$

This is backed up by theoretical(cite) and experimental(cite) results.

2. From Struture Factor

you cannot assign a unique wavevector to individual modes.[43]

Calculating the structure factors of the supercell Gamma modes is a method to test for their plane-wave character at a particular wave vector and polarization corresponding to the VC.[27,46] Feldman et al. used the structure factor to predict an effective dispersion for a model of amorphous silicon, but did not predict group velocities.[27] Volz and Chen used the dynamic structure factor to predict the dispersion of crystalline SW silicon using MD simulation.[47]

which has also been used to determine the dispersion relation from experimentally derived predictions.[48]

The structure factor at a VC wave vector $\boldsymbol{\kappa}_{VC}$ is defined as[46]

$$S^{L,T} = \sum_{\nu} E^{L,T}\delta[\omega - \omega], \tag{22}$$

where the summation is over the Gamma modes, E^T refers to the transverse polarization and is defined as

$$E^L = \left| \sum_b \hat{\boldsymbol{\kappa}}_{VC} \cdot e \exp\left[i\boldsymbol{\kappa}_{VC} \cdot \boldsymbol{r}_0\left(\substack{l=0 \\ b}\right)\right] \right|^2 \tag{23}$$

and E^L refers to the longitudinal polarization and is defined as

$$E^T = \left| \sum_b \hat{\boldsymbol{\kappa}}_{VC} \times e \exp\left[i\boldsymbol{\kappa}_{VC} \cdot \boldsymbol{r}_0\left(\substack{l=0 \\ b}\right)\right] \right|^2. \tag{24}$$

In Eqs. (23) and (24), the b summations are over the atoms in the disordered supercell, $\boldsymbol{r}_0\left(\substack{l=0 \\ b}\right)$ refers to the equilibrium atomic position of atom b in the supercell, l labels the unit cells ($l = 0$ for the supercell), α labels the Cartesian coordinates, and $\hat{\boldsymbol{\kappa}}_{VC}$ is a unit vector. Explicit disorder is included in the Gamma frequencies ω and the $3N_a$ components of the eigenvectors, e.

A frequency and lifetime is predicted by fitting each structure factor peak $S^{L,T}$ to a Lorentzian function

$$S^{L,T} = \sum_{\nu}^{3n} \frac{C_0(\nu)}{[\omega_0(\kappa) - \omega]^2 + \Gamma^2(\nu)}, \tag{25}$$

where $C_0(\nu)$ is a constant related to the DOS.[49]

Fig 4 of this work shows a dispersion extracted by locating the peaks in the structure factor.[50] The dispersion at low frequency is also dominated by transverse sound speed.

Fig. 5 discusses how since the low freq modes are sparse, there is a resonant effect between[27]

The structure factor gives the frequency spectrum needed to construct a (nonstationary) propagating state with a pure wave vector Q and pure longitudinal or transverse polarization[26]. Locations of spectral peaks are peaked like a acoustic dispersion branches. Only low-frequency vibrations have an (approximate) wavevector in disordered systems, and there is no theorem guranteeing this.[27]

It is not possible to identify a unique wavevector for each mode[51]

However, it is very difficult to distinguish between localized and extended modes at high frequencies on the basis of their $S(k, \nu)$ functions, as illustrated by the very similar scattering functions for a 67-meV localized and a 63-meV extended mode in Fig. 3(b).[43]

The dynamic structure factor can be useful for demonstrating the plane-wave character of low-frequency vibrations. However, on a mode-by-mode basis, it is unable in general to characterize a given mode as either localized or delocalized. Thus, it is not possible to

$$\mathbf{v}_{g,\mathbf{n}}\left(\substack{\boldsymbol{\kappa} \\ \nu}\right) = \frac{\partial\omega\left(\substack{\boldsymbol{\kappa} \\ \nu}\right)}{\partial\boldsymbol{\kappa}}. \tag{26}$$

estimates of the sound speeds are found from using finite difference of the peaks in $S_{T,L}$ for different values of k.

The dispersion for a-SiO_2 more closely resembles the so-called "dispersion law for diffusons", where $\omega \propto q^2$.[49]

A group velocity can be assigned by taking a slope of a graph of peak frequency versus wave vector.[26]

$$\mathbf{v}_{g,\mathbf{n}}\left(\substack{\boldsymbol{\kappa} \\ \nu}\right) = \frac{\partial\omega\left(\substack{\boldsymbol{\kappa} \\ \nu}\right)}{\partial\boldsymbol{\kappa}}. \tag{27}$$

Table **??**.

TABLE I: Estimated from the elastic constants, the pre-annealed group velocities are $v_{s,T,} = 3,670$, $v_{s,L,elas} = 7,840$ $v_{s,T,elas} = 2,541$, $v_{s,L,elas} = 4,761$ (see Section).

method	B_{mod} (Eq. (??))	$S_{T,L}$ (Eq. (22), (27))	DOS (Eq. (9))
a-SiO_2			
transverse	3,161	2,732	2,339
longitudinal	5,100	4,779	
a-Si			
transverse	3,886	3,699	3,615
longitudinal	8,271	8,047	

C. Mode Lifetimes

1. From Structure Factor

Ioffe-Regel limit[52].

2. From Normal Mode Decomposition

We use the MD simulation-based NMD method to predict the lifetimes .[53–56] In NMD, the atomic trajectories are first mapped onto the vibrational mode coordinate time derivative,[57]

$$\dot{q}(^{\boldsymbol{\kappa}}_{\nu};t) = \sum_{\alpha,b,l}^{3,n,N} \sqrt{\frac{m_b}{N}} \dot{u}_\alpha\left(^{l}_{b};t\right) e^{*}(^{\boldsymbol{\kappa}\ b}_{\nu\ \alpha}) \exp[i\boldsymbol{\kappa}\cdot\mathbf{r}_0(^{l}_{0})]. \quad (28)$$

Here, m_b is the mass of the b_{th} atom in the unit cell, u_α is the α-component of the atomic displacement from equilibrium, $\dot{u}_\alpha$ is the α-component of the atomic velocity, and t is time.

The spectral energy of each vibrational mode, $\Phi(^{\boldsymbol{\kappa}}_{\nu};t)$, is calculated from

$$\Phi(\boldsymbol{\kappa},\omega) = 2\sum_{\nu}^{3n} T(^{\boldsymbol{\kappa}}_{\nu};\omega) = 2\sum_{\nu}^{3n} \lim_{\tau_0\to\infty} \frac{1}{2\tau_0}\left|\frac{1}{\sqrt{2\pi}}\int_0^{\tau_0} \dot{q}(^{\boldsymbol{\kappa}}_{\nu};t)\exp(-i\omega t)dt\right|^2 \quad (29)$$

The vibrational mode lifetime is predicted by fitting each mode's spectral energy $\Phi(\nu,\omega)$ to a Lorentzian function

$$\Phi(\nu,\omega) = \sum_{\nu}^{3n} \frac{C_0(\nu)}{[\omega_0(\nu)-\omega]^2+\Gamma^2(\nu)}, \quad (30)$$

where the constant $C_0(\nu)$ is related to the average energy of each mode and the linewidth $\Gamma(\nu)$.[56] The mode lifetime is given by

$$\tau(\nu) = \frac{1}{2\Gamma(\nu)} \quad (31)$$

Lifetimes were predicted using anharmonic lattice dynamics, but no thermal transport properties were predicted.[58]

The lifetimes of vibrational modes in a-Si were predicted using normal mode decomposition.[33]

The mode lifetimes show a similar plateau at higher frequencies, particularly for a-Si, which has been reported for disordered lattices.[59]

We find that the diffusivity 15 displays a well-defined kink at a frequency d that separates the low regime of divergent diffusivity consistent with Rayleigh law from a character- istic plateau that persists up to high where localization sets in.[50]

In conclusion, we have found that the high-frequency VS in a realistic model of amorphous Si decay on picosecond time scales, and at low temperatures their lifetimes de- crease as frequency increases. This is in contrast to recent experimental claims that the modes decay on nanosecond scales and their lifetimes increase as frequency increases.[58]

The lifetimes found by this method are in good agreement with the perturbative calculations of Fabian and Allen and are on the order of 10 ps at low tem- peratures in both 216 and 4096 atom supercells.[60]

Our results indicate that all of these processes occur on a much faster time scale than the 1 ns temporal resultion of the Raman experiments, so it is not obvious that the measured relaxation rates should be identified with vibrational lifetimes.[61]

"The modes of mixed character which lie outside or in between the central groups of pure plane-wave modes are typically resonances as indicated by the large values of 1/p i . How- ever, these modes are also reasonably well interpreted as filling in the appropriate tails of Lorentzian response func- tions, modulo small statistical fluctuations to be expected in finite systems. bigger and small Q s become less sparse, Lorentzians of fixed width will overlap increasingly, and can force out the resonant states which otherwise would inhabit the gaps. For Q of order 1/L there will always be gaps, no matter how big the system L see for instance the region near 4.1 meV in Fig. 2 where a resonance occurs, but these gaps drift toward Q 0 and 0 as L increases. Therefore the distinction between special frequencies lying in gaps, and other frequen- cies lying in Lorentzian peaks, must disappear as L increases. There are two possibilities: either resonant behavior entirely disappears, or else it remains in a diluted form and is shared uniformly by all the normal modes. That is, at any given frequency there may be isolated parts of a large sample which are particularly sensitive to oscillation at just this fre- quency and temporarily trap selected traveling waves of this frequency. If this behavior is found for all normal modes, then any one normal mode will be freely propagating almost everywhere, and it becomes a subtle matter of definition or taste whether they should be called resonances at all. "s

"To implement Eq. 6 one must know the correct Q dependence of Q . As shown in Fig. 8, the fitted values scatter too much to guide the extrapolation well. In principle, at very small Q one should get a form Q CQ 4 which corresponds to Rayleigh scattering of sound waves from the structural disorder. The data of Fig. 8 do not fit a Q 4 law; the Q 2 curve shown in the figure is a

better fit. Two experiments13,15 but not a third35 and one calculation18 on a-SiO2 have also given Q 2 . We do not know a theory which can give this law in a harmonic model.

"The conclusion is that intrinsic harmonic glassy disorder contained in our finite calculation kills off the heat-carrying ability of propagons rapidly enough without invoking any exotic mechanism. Our (T) curve is reminiscent of the ex- periments of Zaitlin and Anderson after holes are introduced to enhance the elastic damping of long-wavelength modes. The plateau disappears from their data in much the same way that it disappears from our theory due to extra damping of small-Q propagons.

scattering from static imperfections would predicts Rayleigh type scattering[62]

D. Diffusivities

This supports the idea of Slack for a-SiO_2[63] While the thermal conductivity of a-SiO , the material is characterized by a constant similar for other amorphous materials such as Lennard-Jones argon[59] and a model of a-GeTe.[64]

Thermal diffusivity was predicted for a percolation network which showed Rayleigh type scattering dependance in the low-frequency limit.[65]

which generally agree with diffusivities computed according to the formula of Edwards and THoules.[27,49,66]

Thermal diffusivity has been predicted using a wave-packet method

It was shown

Garber shows that these high-frequency modes are localized in the Anderson sense, showing exponential decay of the mode eigenvector.[67]

It was shown that the diffusivity $D_{AF}(\omega) \propto DOS(\omega)$ at low frequency when the modes are spatially uncorrelated and the overlap between them is small and independent of the frequency.[50,68]

At low frequencies, the AF-predicted and NMD-predicted mode diffusivities scale as $D \propto \omega^{-2}$, similar to the scaling due to Umklapp scattering of phonons in a crystalline system. Rayleigh scattering due to point defects predicts $D \propto \omega^{-4}$, but is not observed in the amorphous systems studied in this work.(cite) While Rayleigh-type scaling has been observed in harmonic studies of the diffusivities of modes in disordered lattics and jammed systems,[50,65,68] it has been demonstrated that the harmonic disorder in a-Si produces a scaling similar to Umklapp scattering.[26]

In summary, we obtain a frequency-independent diffusiv- ity when the density of states is frequency-independent and the following conditions are satisfied: A displacements of particles in different modes of similar frequency are uncor- related; B the directions of changes in the relative displace- ments of pairs of interacting particles are spatially uncorre- lated within a given mode; and C the direction of change in the relative displacement

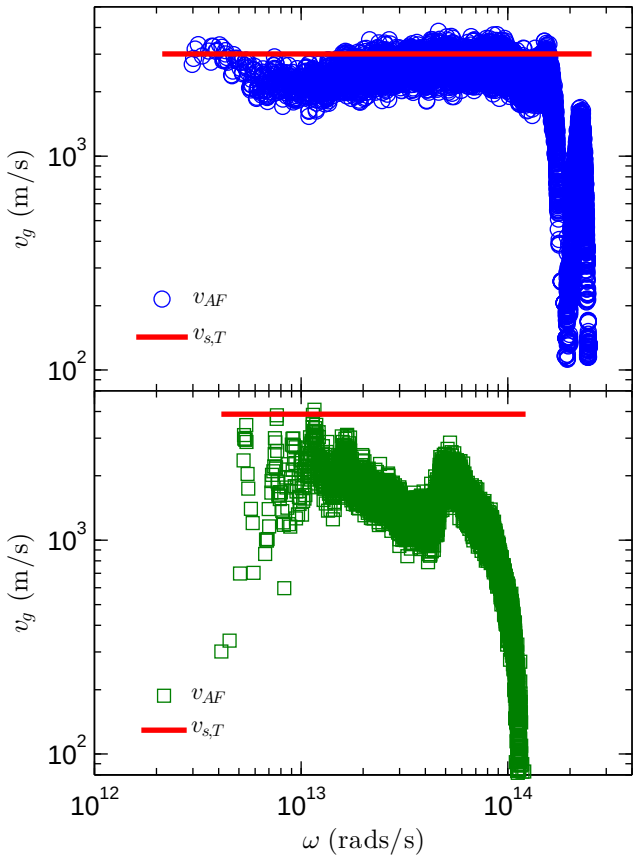

FIG. 1: .

of a pair of interacting particles is uncorrelated from the direction of the displacement.

Both a-SiO_2 and a-Si have a region at higher frequencies where the AF-predicted mode diffusivities are relatively constant. This behavior has been reported for a number of disordered systems such as disordered lattices[49,59,65] and jammed systems. At the higest frequencies the AF-predicted diffusivities trend exponentially to zero, which is an indication that these modes are "locons", spatially localized modes which do not contribute to thermal condutivity.[46]

This perplexing property of glasses has been explained heuristically by assuming that phonons are scattered so strongly by structural disorder that trans- port becomes diffusive, with a frequency regime of small, constant thermal diffusivity.[65,69?]

$$v_{AF} = \frac{D_i}{2\Gamma(\nu)} \tag{32}$$

E. Mean Free Paths

Using the lifetimes predicted from the structure factor peaks and the transverse sound speed, the MFP is about the size of the simulation cell L.

VII. THERMAL CONDUCTIVITY

A. Bulk

Lee found a value of around 1 W/m-K but with very small supercell sizes.[70]

We use the GK method to predict the thermal conductivity. The GK method is relatively inexpensive compared to the NMD and AF methods so that large system sizes can be simulated (see Section).

For smaller system sizes, the same trajectories are used for the GK and NMD methods. The MD simulations were run with the same parameters as the NMD metho (see Section).

The predicted thermal condcutivties from the GK method are plotted in Fig. . For a-SiO2, the thermal conductivity is size independent within the errors. For a-Si, there is a clear size-dependance of the thermal conductivity

To compare the results of the mode-based methods (NMD and AF) and the GK method, it is necessary to estimate the missing contribution from vibrational modes with frequency less than the minimum frequency of the finnite systems.

Assuming the thermal conductivity form Eq. for the lowest frequency modes in the system, the thermal conductivity as a function of the system size takes the form

$$\frac{k(N_0)}{k_{bulk}} = 1 - \frac{c_0}{N_0}, \tag{33}$$

"We find that we cannot define a wave vector for the majority of the states, but the intrinsic harmonic diffusivity is still well-defined and has a numerical value similar to what one gets by using the Boltzmann result, replacing v by a sound velocity and replacing l by an interatomic distance a. "[26]

"In order to fit the experimental sc(T) it is necessary to add a Debye- like continuation from 10 meV down to 0 meV. The harmonic diffusivity becomes a Rayleigh m law and gives a divergent (T) as T O. To eliminate this we make the standard assumption of resonant- plus-relaxational absorption from two-level systems (this is an anharmonic effect which would lie outside our model even if it did contain two-level systems implicitly). "[26]

Debye model. $k_{tot} = k_{phonon} + k_A$ $F. For lack of a rigorous definition of phonon vs diffusion, we will define k_{phonon} as the k_{debye}.

The relative contribution of k_{phonon} and k_A $Fis also predicted to be similar for silicon nanoufilms.[45]

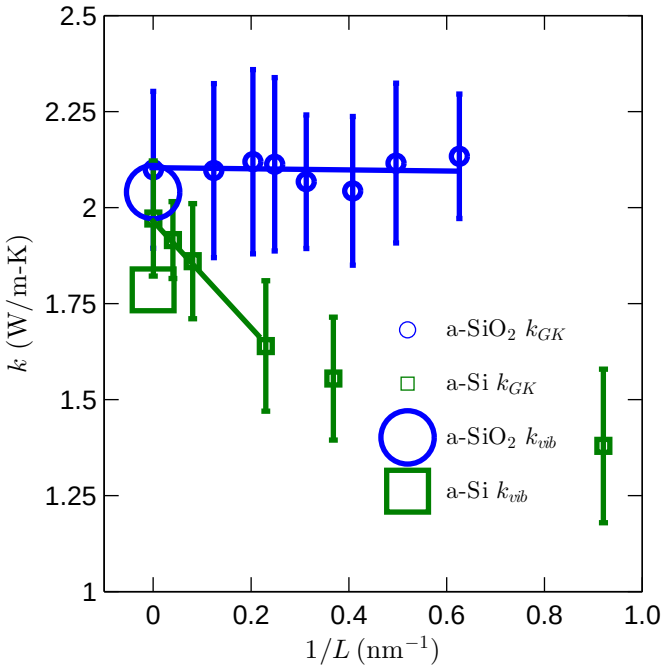

B. Accumulation

C. Discussion

This agress with previous estimates for the contribution of low frequency ($\omega < 30 rads/s$)[71]

Moedling shows that alloying a-Si with Ge can further reduce the thermal conductivity of the bulk and thin films.[26,72]

The agree- ment between the 3! and the TDTR measurements at 1.11 MHz suggests that phonons with ¿ D=!1=2 14 612 nm are not significant for thermal conduction in this sample. Furthermore, the difference between the high and low frequency measurements by TDTR indicates that pho- nons with 162 ¡ ¡ 612 nm contribute 40% of the of the sample.[22]

The acoustic projected spectral density SQ; E is shown in Fig. 3. From the Q 14 h100i transverse and longitudinal projections, we obtain the respective phase velocities of vt = 4,740 v_l = 7,830 m/s Wooten model, where v_t is significantly higher than the value for our a-Si model (see Table).[22]

Even though the DOS of the WWW produced structures compare well with other models and also experimental measurements, it has been demonstrated that the spectral properties at low frequency can be much different, particularly the linewdith of the structure factor.[22] It is possible that the

Based on the variation of thermal conductivity with film thickness, Liu et al also report a MFP scaling of

$\Lambda \propto \omega^{-2}$.[22] Similar experimental results were obtained for a-SiO_2.[73]

Tight-binding models for a-Si can improve the low-frequency DOS prediction compared to experiment.[74]

A combination of frequency-domain, time-domain, and variable physical heating size measurments would be helpful in investigating[13,24,29,75]

VIII. SUMMARY

Table **??**.

[1] D. G. Cahill, W. K. Ford, K. E. Goodson, G. D. Mahan, A. Majumdar, H. J. Maris, R. Merlin, and S. R. Phillpot, Journal of Applied Physics **93**, 793818 (2003).

[2] J.-K. Yu, S. Mitrovic, D. Tham, J. Varghese, and J. R. Heath, Nature Nanotechnology **5**, 718721 (2010).

[3] A. I. Hochbaum, R. Chen, R. D. Delgado, W. Liang, E. C. Garnett, M. Najarian, A. Majumdar, and P. Yang, Nature **451**, 163167 (2008).

[4] G. Pernot, M. Stoffel, I. Savic, F. Pezzoli, P. Chen, G. Savelli, A. Jacquot, J. Schumann, U. Denker, I. Mnch, et al., Nat Mater **9**, 491 (2010), ISSN 1476-1122, URL http://dx.doi.org/10.1038/nmat2752.

[5] A. I. Boukai, Y. Bunimovich, J. Tahi-Kheli, J.-K. Yu, W. A. G. Goddard, and J. R. Heath, Nature **451**, 168171 (2008).

[6] B. Poudel, Q. Hao, Y. Ma, Y. Lan, A. Minnich, B. Yu, X. Yan, D. Wang, A. Muto, D. Vashaee, et al., Science **320**, 634638 (2008), URL http://www.sciencemag.org/content/320/5876/634.abstract.

[7] G. D. Mahan and F. Claro, Phys. Rev. B **38**, 19631969 (1988), URL http://link.aps.org/doi/10.1103/PhysRevB.38.1963.

[8] G. Chen, Journal of Nanoparticle Research **2**, 199 (2000), ISSN 1388-0764, URL http://dx.doi.org/10.1023/A%3A1010003718481.

[9] M. G. Holland, Physical Review **132**, 2461 (1963).

[10] A. Ward and D. A. Broido, Phys. Rev. B **81**, 085205 (2010), URL http://link.aps.org/doi/10.1103/PhysRevB.81.085205.

[11] A. D. Christianson, M. D. Lumsden, O. Delaire, M. B. Stone, D. L. Abernathy, M. A. McGuire, A. S. Sefat, R. Jin, B. C. Sales, D. Mandrus, et al., Phys. Rev. Lett. **101**, 157004 (2008), URL http://link.aps.org/doi/10.1103/PhysRevLett.101.157004.

[12] M. Highland, B. C. Gundrum, Y. K. Koh, R. S. Averback, D. G. Cahill, V. C. Elarde, J. J. Coleman, D. A. Walko, and E. C. Landahl, Phys. Rev. B **76**, 075337 (2007), URL http://link.aps.org/doi/10.1103/PhysRevB.76.075337.

[13] Y. K. Koh and D. G. Cahill, Phys. Rev. B **76**, 075207 (2007), URL http://link.aps.org/doi/10.1103/PhysRevB.76.075207.

[14] J. J. Freeman and A. C. Anderson, Physical Review B **34**, 5684\textbackslashtextbackslashtextbackslash965690 (1986).

[15] D. G. Cahill, S. K. Watson, and R. O. Pohl, Phys. Rev. B **46**, 61316140 (1992), URL http://link.aps.org/doi/10.1103/PhysRevB.46.6131.

[16] H. Wada and T. Kamijoh, Japanese Journal of Applied Physics **35**, L648L650 (1996), URL http://jjap.jsap.jp/link?JJAP/35/L648/.

[17] B. L. Zink, R. Pietri, and F. Hellman, Physical Review Letters **96**, 055902 (2006), URL http://link.aps.org/doi/10.1103/PhysRevLett.96.055902.

[18] H.-S. Yang, D. G. Cahill, X. Liu, J. L. Feldman, R. S. Crandall, B. A. Sperling, and J. R. Abelson, Phys. Rev. B **81**, 104203 (2010), URL http://link.aps.org/doi/10.1103/PhysRevB.81.104203.

[19] D. G. Cahill, M. Katiyar, and J. R. Abelson, Physical Review B **50**, 60776081 (1994).

[20] B. S. W. Kuo, J. C. M. Li, and A. W. Schmid, Applied Physics A: Materials Science & Processing **55**, 289296 (1992), ISSN 0947-8396, 10.1007/BF00348399, URL http://dx.doi.org/10.1007/BF00348399.

[21] S. Moon, M. Hatano, M. Lee, and C. P. Grigoropoulos, International Journal of Heat and Mass Transfer **45**, 2439 2447 (2002), ISSN 0017-9310, URL http://www.sciencedirect.com/science/article/pii/S0017931001003477.

[22] X. Liu, J. L. Feldman, D. G. Cahill, R. S. Crandall, N. Bernstein, D. M. Photiadis, M. J. Mehl, and D. A. Papaconstantopoulos, Phys. Rev. Lett. **102**, 035901 (2009), URL http://link.aps.org/doi/10.1103/PhysRevLett.102.035901.

[23] L. Wieczorek, H. Goldsmid, and G. Paul, in *Thermal Conductivity 20*, edited by D. Hasselman and J. Thomas, J.R. (Springer US, 1989), pp. 235–241, ISBN 978-1-4612-8069-9, URL http://dx.doi.org/10.1007/978-1-4613-0761-7_22.

[24] A. J. Minnich, J. A. Johnson, A. J. Schmidt, K. Esfarjani, M. S. Dresselhaus, K. A. Nelson, and G. Chen, Phys. Rev. Lett. **107**, 095901 (2011), URL http://link.aps.org/doi/10.1103/PhysRevLett.107.095901.

[25] F. Yang and C. Dames, Physical Review B **87**, 035437 (2013), URL http://link.aps.org/doi/10.1103/PhysRevB.87.035437.

[26] J. L. Feldman, M. D. Kluge, P. B. Allen, and F. Wooten, Physical Review B **48**, 1258912602 (1993).

[27] J. L. Feldman, P. B. Allen, and S. R. Bickham, Phys. Rev. B **59**, 35513559 (1999), URL http://link.aps.org/doi/10.1103/PhysRevB.59.3551.

[28] Y. He, D. Donadio, J.-H. Lee, J. C. Grossman, and G. Galli, ACS Nano **5**, 1839\textbackslashtextbackslashtextbackslashtextbackslashtextbackslashtextbacksla (2011).

[29] K. T. Regner, D. P. Sellan, Z. Su, C. H. Amon, A. J. McGaughey, and J. A. Malen, Nat Commun **4**, 1640 (2013), URL http://dx.doi.org/10.1038/ncomms2630.

[30] S.-M. Lee and D. G. Cahill, Journal of Applied Physics **81**, 25902595 (1997).

[31] T. Yamane, N. Nagai, S.-i. Katayama, and M. Todoki, Journal of Applied Physics **91**, 97729776 (2002), URL http://link.aip.org/link/?JAP/91/9772/1.

[32] P. B. Allen and J. L. Feldman, Physical Review B **48**, 1258112588 (1993).

[33] Y. He, D. Donadio, and G. Galli, Applied Physics Letters **98**, 144101 (2011), URL http://link.aip.org/link/?APL/98/144101/1.

[34] J. M. Ziman, *Electrons and Phonons* (Oxford, New York, 2001).

[35] D. Cahill and R. Pohl, Annual Review of Physical Chemistry **39**, 93121 (1988).

[36] G. T. Barkema and N. Mousseau, Phys. Rev. B **62**, 49854990 (2000), URL http://link.aps.org/doi/10.1103/PhysRevB.62.4985.

[37] S. Plimpton, Journal of Computational Physics **117**, 1 19 (1995), ISSN 0021-9991, URL http://www.sciencedirect.com/science/article/pii/S002199918571039X.

[38] J. D. Gale and A. L. Rohl, Molecular Simulation **29**, 291 (2003).

[39] R. O. Pohl, X. Liu, and E. Thompson, Rev. Mod. Phys.

74, 9911013 (2002), URL http://link.aps.org/doi/10.1103/RevModPhys.74.991.

[40] W. Senn, G. Winterling, M. Grimsditch, and M. Brodsky, in *Inst. Phys. Conf. Ser* (1979), p. 709.

[41] R. Vacher, H. Sussner, and M. Schmidt, Solid State Communications **34**, 279 (1980), ISSN 0038-1098, URL http://www.sciencedirect.com/science/article/pii/0038109880905578.

[42] J. L. Feldman, J. Q. Broughton, and F. Wooten, Phys. Rev. B **43**, 21522158 (1991), URL http://link.aps.org/doi/10.1103/PhysRevB.43.2152.

[43] R. Biswas, A. M. Bouchard, W. A. Kamitakahara, G. S. Grest, and C. M. Soukoulis, Phys. Rev. Lett. **60**, 22802283 (1988), URL http://link.aps.org/doi/10.1103/PhysRevLett.60.2280.

[44] J. C. Duda, T. S. English, D. A. Jordan, P. M. Norris, and W. A. Soffa, Journal of Physics: Condensed Matter **23**, 205401 (2011), URL http://stacks.iop.org/0953-8984/23/i=20/a=205401.

[45] D. Donadio and G. Galli, Phys. Rev. Lett. **102**, 195901 (2009).

[46] P. B. Allen, J. L. Feldman, J. Fabian, and F. Wooten, Philosophical Magazine B **79**, 17151731 (1999).

[47] S. Volz and G. Chen, Physical Review B **61**, 26512656 (2000).

[48] N. L. Green, D. Kaya, C. E. Maloney, and M. F. Islam, Physical Review E **83**, 051404 (2011), URL http://link.aps.org/doi/10.1103/PhysRevE.83.051404.

[49] Y. M. Beltukov, V. I. Kozub, and D. A. Parshin, Phys. Rev. B **87**, 134203 (2013), URL http://link.aps.org/doi/10.1103/PhysRevB.87.134203.

[50] V. Vitelli, N. Xu, M. Wyart, A. J. Liu, and S. R. Nagel, Phys. Rev. E **81**, 021301 (2010), URL http://link.aps.org/doi/10.1103/PhysRevE.81.021301.

[51] L. E. Silbert, A. J. Liu, and S. R. Nagel, Phys. Rev. E **79**, 021308 (2009), URL http://link.aps.org/doi/10.1103/PhysRevE.79.021308.

[52] S. N. Taraskin and S. R. Elliott, Philosophical Magazine Part B **79**, 17471754 (1999), URL http://www.tandfonline.com/doi/abs/10.1080/13642819908223057.

[53] A. J. C. Ladd, B. Moran, and W. G. Hoover, Physical Review B **34**, 50585064 (1986).

[54] A. J. H. McGaughey and M. Kaviany, Physical Review B **69**, 094303 (2004).

[55] J. E. Turney, E. S. Landry, A. J. H. McGaughey, and C. H. Amon, Phys. Rev. B **79**, 064301 (2009), URL http://link.aps.org/doi/10.1103/PhysRevB.79.064301.

[56] J. M. Larkin, J. E. Turney, A. D. Massicotte, C. H. Amon, and A. J. H. McGaughey, to appear in Journal of Computational and Theoretical Nanoscience (2012).

[57] M. T. Dove, *Introduction to Lattice Dynamics* (Cambridge, Cambridge, 1993).

[58] J. Fabian and P. B. Allen, Phys. Rev. Lett. **77**, 38393842 (1996), URL http://link.aps.org/doi/10.1103/PhysRevLett.77.3839.

[59] J. Larkin and A. McGaughey, Journal of Applied Physics (2013).

[60] S. R. Bickham and J. L. Feldman, Phys. Rev. B **57**, 1223412238 (1998), URL http://link.aps.org/doi/10.1103/PhysRevB.57.12234.

[61] S. R. Bickham, Phys. Rev. B **59**, 48944897 (1999), URL http://link.aps.org/doi/10.1103/PhysRevB.59.4894.

[62] P. G. Klemens, Proceedings of the Physical Society. Section A **68** (1955).

[63] G. A. Slack (Academic Press, 1979), vol. 34 of *Solid State Physics*, p. 1 71, URL http://www.sciencedirect.com/science/article/pii/S0081194708603598.

[64] G. C. Sosso, D. Donadio, S. Caravati, J. Behler, and M. Bernasconi, Phys. Rev. B **86**, 104301 (2012), URL http://link.aps.org/doi/10.1103/PhysRevB.86.104301.

[65] P. Sheng and M. Zhou, Science **253**, 539542 (1991), URL http://www.sciencemag.org/content/253/5019/539.abstract.

[66] J. T. Edwards and D. J. Thouless, Journal of Physics C: Solid State Physics **5**, 807 (1972), URL http://stacks.iop.org/0022-3719/5/i=8/a=007.

[67] W. Garber, F. M. Tangerman, P. B. Allen, and J. L. Feldman, Philosophical Magazine Letters **81**, 433439 (2001), URL http://www.tandfonline.com/doi/abs/10.1080/09500830110041666.

[68] N. Xu, V. Vitelli, M. Wyart, A. J. Liu, and S. R. Nagel, Phys. Rev. Lett. **102**, 038001 (2009), URL http://link.aps.org/doi/10.1103/PhysRevLett.102.038001.

[69] C. Kittel, Physical Review **75**, 974 (1949).

[70] Y. H. Lee, R. Biswas, C. M. Soukoulis, C. Z. Wang, C. T. Chan, and K. M. Ho, Phys. Rev. B **43**, 65736580 (1991), URL http://link.aps.org/doi/10.1103/PhysRevB.43.6573.

[71] M. S. Love and A. C. Anderson, Phys. Rev. B **42**, 18451847 (1990), URL http://link.aps.org/doi/10.1103/PhysRevB.42.1845.

[72] A. M. Bouchard, R. Biswas, W. A. Kamitakahara, G. S. Grest, and C. M. Soukoulis, Phys. Rev. B **38**, 1049910506 (1988), URL http://link.aps.org/doi/10.1103/PhysRevB.38.10499.

[73] C. Masciovecchio, G. Baldi, S. Caponi, L. Comez, S. Di Fonzo, D. Fioretto, A. Fontana, A. Gessini, S. C. Santucci, F. Sette, et al., Phys. Rev. Lett. **97**, 035501 (2006), URL http://link.aps.org/doi/10.1103/PhysRevLett.97.035501.

[74] J. L. Feldman, N. Bernstein, D. A. Papaconstantopoulos, and M. J. Mehl, Phys. Rev. B **70**, 165201 (2004), URL http://link.aps.org/doi/10.1103/PhysRevB.70.165201.

[75] M. E. Siemens, Q. Li, R. Yang, K. A. Nelson, E. H. Anderson, M. M. Murnane, and H. C. Kapteyn, Nature Materials **9**, 2630 (2010).